

Online Supporting Information for

Active stereo-control of the Cl + CH₄($\nu_3=1$) reaction: A three-dimensional perspective

Huilin Pan,^{1,2*} Kopin Liu^{1,3,4*}

¹ Institute of Atomic and Molecular Sciences (IAMS), Academia Sinica, P. O. Box 23-166,
Taipei, Taiwan 10617.

² Southern University of Science and Technology, Shenzhen, P. R. China.

³ State Key Laboratory of Molecular Reaction Dynamics, Dalian Institute of Chemical Physics,
CAS, Dalian 116023, P. R. China.

⁴ Aerosol Science Research Center, National Sun Yat-sen University, Kaohsiung, Taiwan 80424.

* To whom correspondence should be addressed, Email: panhl2019@sustech.edu.cn (H.P.);
kliu@po.iams.sinica.edu.tw (K.L.)

This PDF file includes:

1. Experimental details
2. What is the PDDCS?
3. Alignments of various internal angular momenta

References

Figs. S1 to S6

1. Experimental details

The details of the rotating-sources, crossed-beam apparatus, and experimental methods have been described in previous reports.¹⁻³ Briefly, two doubly skimmed, pulsed beams (a discharge-generated Cl-atom beam from a mixture of 5% Cl₂ in Ne at 6 bar, and a neat CH₄ beam also at 6 bar) were crossed in the center of a time-sliced and velocity-mapped ion-imaging setup housed in a differentially pumped chamber. Two pulsed lasers, an infrared optical parametric oscillator/amplifier (IR OPO/A) pump and an ultraviolet (UV) probe, were directed perpendicularly to each other and in the same plane as the two molecular beams. All four beams crossed in the collision region, with the IR laser offset a few mm upstream for building up the product yields. A small fraction (few %) of the excited CH₄($v_3=1$, $|jM| = |101\rangle$) reactant was pumped by the IR laser tuned to the R(0) transition at 3028.75 cm⁻¹.^{4,5} A variable wave-plate was exploited to alter the IR-polarization (\mathcal{E}_{IR}) direction, thus manipulating the aligned CH₄ in the scattering frame. After the collisions, the ground state CH₃(0₀) products were detected by a (2+1) resonance-enhanced multiphoton ionization (REMPI) method⁶ and recorded by a time-sliced, velocity-mapped image. For experimental reasons, the probe laser wavelength was fixed at the peak of the Q-head of CH₃(0₀) REMPI band, which mainly detected the low- j states of CH₃(0₀) products. Test experiments with the probe laser wavelength tuned off the REMPI peak, which then primarily sampled the higher j -states of CH₃(0₀), indicated very small differences in the polarized images. Similar findings were quantitatively reported in a recent study on the Cl + CHD₃($v_1=1$) reaction.⁷

For each day's experiment, a given molecular beam geometry at an E_c was chosen and product images were acquired at three to four different IR-polarization configurations. Images of each IR-polarization configuration (and that with IR-off for subtracting the ground-state and bend-excited reaction signals) were recorded at 20 Hz for 5 minutes in sequence, and this cycle was then repeated 10-15 times for signal accumulations. The parameters needed for the density-to-flux correction, such as the temporal overlaps of two molecular beams (both IR-on and IR-off) and UV laser focusing conditions etc., were measured at the end of each day's experiment. Experiments under each molecular-beam geometry were also repeated 2-3 times at different days for consistent check and for generating the final set of product images presented in this report.

2. What is the PDDCS?

The physical meanings of the four PDDCSs are briefly outlined.^{8,9} The $S_0^0(\theta)$ represents the 2-dimensional (2D) angular distribution in the scattering plane for unpolarized (i.e., randomly oriented) reactants. In this 2D analysis of the sliced images, the intensity of each pixel is weighted by its center-of-mass speed u (instead of u^2 in the 3D analysis) and without the solid angle factor $\sin\theta$. The remaining three polarization moments $S_{q+}^2(\theta)$ quantify perturbations, resulting from a given reactant polarization preparation as \mathcal{E}_{IR} set at (α, Φ) , to the unpolarized DCS $S_0^0(\theta)$. Summarized below is how the signs of the $S_{q+}^2(\theta)$ moments give the directional propensity for reactivity as a function of the reactant \mathbf{j} -alignment. A positive (negative) value of $S_0^2(\theta)$ indicates the propensity of the \mathbf{j} -vector pointing along (perpendicular to) the \mathbf{k} -vector (the $\pm z$ -axis). The value of $S_{1+}^2(\theta)$ gauges the tilting of the \mathbf{j} -vector with respect to the xy and yz planes with a positive sign for \mathbf{j} tilting toward $\pm (x+z)$ and negative toward $\pm (x-z)$. The value of $S_{2+}^2(\theta)$ indicates the propensity of the \mathbf{j} being parallel to the $\pm x$ -axis (a positive value) or to the $\pm y$ -axis (a negative value).

3. Alignment of various internal angular momenta

The key to understand the polarized scattering experiment is to have clear distinctions of the directional properties of internal angular momenta of the polarized reactant in two different frames: the molecule-fixed and laboratory-fixed frames. A bulk of the following discussion has been given in several previous reports.^{3,10-12}

In short, for a spherical-top reactant such as $\text{CH}_4(\nu_3=1)$, since $l = 1$ for $\nu_3 = 1$ and $\mathbf{j} = \mathbf{N} + \mathbf{l}$, N can take on three values of $j-1$, j , and $j+1$, corresponding to \mathbf{l} being parallel, perpendicular, and anti-parallel to \mathbf{j} in the classical vector model. The degeneracy of three states will be lifted by the Coriolis interactions, leading to the three energy levels of $F^-(j)$, $F^0(j)$ and $F^+(j)$ for the R-, Q-, and P-branches, respectively. Among the three split states, the state $F^0(j)$, with \mathbf{l} being perpendicular to \mathbf{j} , does not change the frequency. The other two, $F^-(j)$ and $F^+(j)$ with \mathbf{l} being parallel or anti-parallel to \mathbf{j} , are linear combinations of the original two vibrations, and thereby execute in-phase excitations constituting an ensemble of elliptical oscillations (one clockwise and the other counter-clockwise). In physical term, the $\text{CH}_4(\nu_3=1)$ molecule prepared by the R-branch excitation shapes as an ellipsoid with all four H atoms uniformly distributed over the surface. For the prepared state $|jNl\rangle = |101\rangle$ of this work, because $N=0$, the excited molecule has no physical rotation and its angular momentum (\mathbf{j}) polarization corresponds purely to the polarization of the vibrational

angular momentum or the alignment of the vibrational amplitude (or displacement vector), $\mathbf{j} // \mathbf{l}$. The above picture depicts the relative directions of \mathbf{j} , \mathbf{N} , and \mathbf{l} in a molecule-fixed (or body-fixed) frame.

When CH₄ is excited ($\nu_3 = 1 \leftarrow 0$) by a linearly polarized IR laser in the laboratory, the electric field \mathcal{E}_{IR} aligns the transition dipole moment \mathbf{d} in space, $\mathbf{d} // \mathcal{E}_{\text{IR}}$. The Coriolis constant $\mathcal{S}_3 (= 0.055)$ for CH₄($\nu_3=1$) has a positive value,¹² and thus the direction of rotation of \mathbf{d} during the vibration coincides with the vibrational angular momentum \mathbf{l} , i.e., $\mathbf{l} \perp \mathbf{d}$ (or \mathcal{E}_{IR}). For the R-branch transition, since $\mathbf{l} // \mathbf{j}$ in the molecule-fixed frame, then $\mathbf{j} \perp \mathcal{E}_{\text{IR}}$ (or \mathbf{d}) in the laboratory-fixed frame. The same conclusion can be reached more elegantly from the polarization selection rule of $\Delta m_j = 0$ (but not allowed for $\Delta j = 0$ and $m = 0$),¹² where the quantization axis refers to the \mathcal{E}_{IR} axis. Thereby, when CH₄($\nu_3=1$) is excited by the R-branch transition, its rotational angular momentum \mathbf{j} possesses the same directional property as CHD₃($\nu_1=1, |10\rangle$) in space, i.e., both are preferentially aligned in a plane perpendicular to \mathcal{E}_{IR} . In contrast, for CHD₃($\nu_1=1, |1\pm 1\rangle$) excited by the Q-branch, its \mathbf{j} will be aligned in parallel to \mathcal{E}_{IR} in the laboratory.

To sum up, in a polarized scattering experiment the reactant is aligned in the laboratory by \mathcal{E}_{IR} via \mathbf{d} . However, in the molecule-fixed frame one has $\mathbf{l} // \mathbf{j} \perp \mathbf{d}$ for CH₄($\nu_3=1$) excited via the R-branch transition and $\mathbf{j} \perp \mathbf{d}$ ($\mathbf{j} // \mathbf{d}$) for the $K = 0$ ($K = \pm 1$) state of CHD₃($\nu_1=1$). In other words, the optical alignments of reactant angular momentum \mathbf{j} can be distinct, depending on the rotational sublevel K or l (or its projection on the figure axis, more precisely). Since the intrinsic reaction dynamics of the rotational sublevels can be different, the projection of \mathbf{j} onto the vibrational amplitude or the displacement vector \mathbf{d} in the molecule-fixed frame should be of the primary concern for understanding the intrinsic polarization moments, PDDCSs.

References

- 1 J. J. Lin, J. Zhou, W. Shiu and K. Liu, *Rev. Sci. Instrum.*, 2003, **74**, 2495-2500.
- 2 F. Wang, J.-S. Lin and K. Liu, *J. Chem. Phys.*, 2014, **140**, 084202.
- 3 H. Pan, J. Yang, F. Wang and K. Liu, *J. Phys. Chem. Lett.*, 2014, **5**, 3878–3883.
- 4 S. Albert, S. Bauerecker, V. Boudon, L. R. Brown, J.-P. Champion, M. Loete, A. Nikitin and M. Quack, *Chem. Phys.*, 2009, **356**, 131-146.
- 5 L. S. Rothman et al., *J. Quant. Spectrosc. Radiat. Transfer*, 2013, **130**, 4-50.

- 6 H. Pan and K. Liu, *J. Chem. Phys.*, 2018, **148**, 014303.
 7 H. Pan, O. Tkac and K. Liu, *J. Chem. Phys.*, 2018, **148**, 244307.
 8 F. Wang, K. Liu and T. P. Rakitzis, *Nat. Chem.* 2012, **4**, 636-641.
 9 J. Aldegunde, M. P. de Miranda, J. M. Haigh, B. K. Kendrick, V. Sáez Rábanos and F. J. Aoiz,
 5 *J. Phys. Chem. A*, 2005, **109**, 6200-6217.
 10 H. Pan, Y. Cheng and K. Liu, *J. Phys. Chem. A*, 2016, 120, 4799–4804.
 11 F. Wang and K. Liu, *J. Chem. Phys.*, 2016, **145**, 144305.
 12 G. H. Herzberg, *Infrared and Raman Spectra of Polyatomic Molecules*, Van Nostrand
 Reinhold, New York, 1945.

10

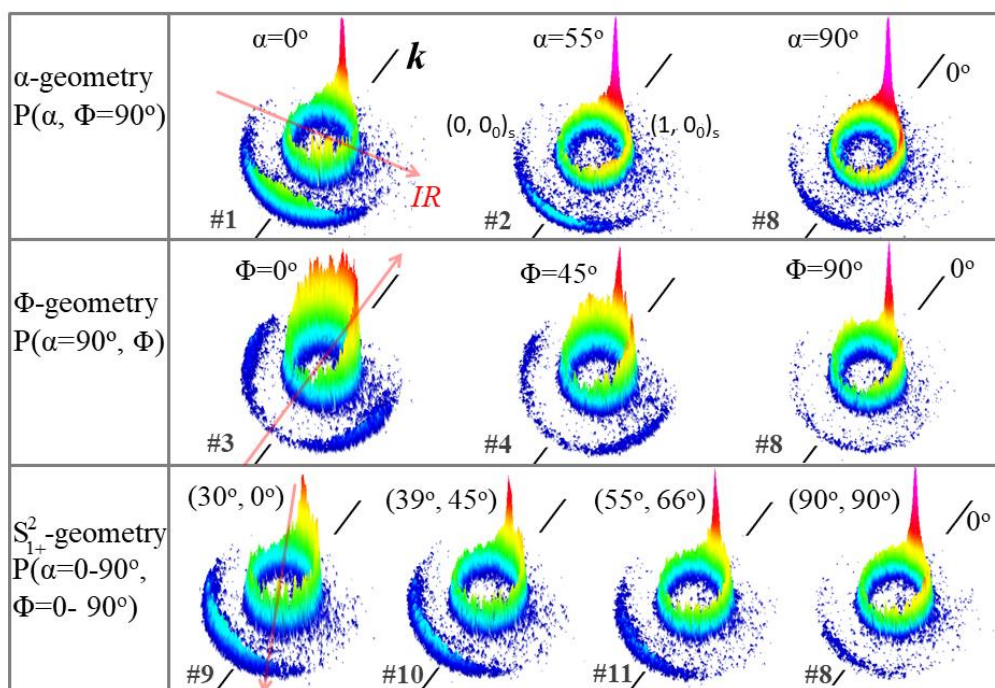


FIG. S1. Same as Fig. 2, except for $E_c = 2.7 \text{ kcal mol}^{-1}$.

15

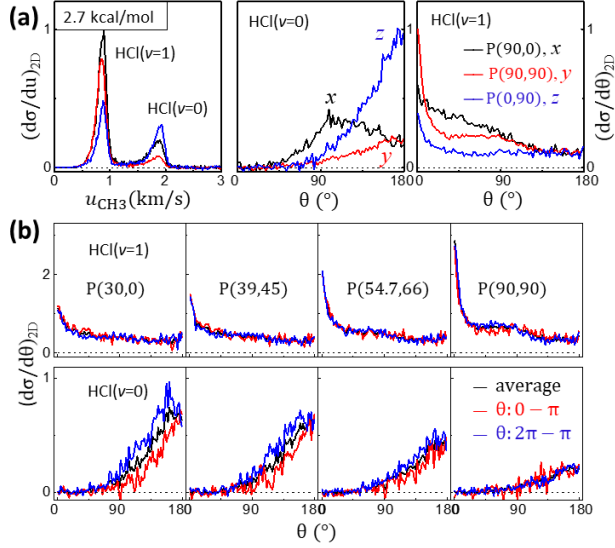


FIG. S2. Same as Fig. 3, except for $E_c = 2.7 \text{ kcal mol}^{-1}$.

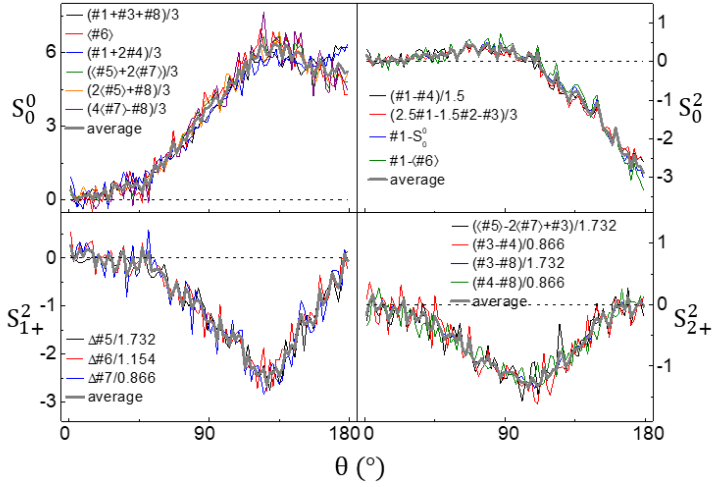


FIG. S3. Demonstration of the inversion method, which exploits various linear combinations of a set of image data, to unfold the individual PDDCS for the HCl($v=0$) product channel at $E_c = 4.8 \text{ kcal mol}^{-1}$. The “#” in each panel refers to the first entry in Table 1; that with the bracket sign, such as $\langle \#5 \rangle$, means the average of the two hemispheres under the #5 polarization configuration, and $\Delta \langle \#5 \rangle$ means the difference between the two hemispheres of $0-\pi$ and $2\pi-\pi$. All image data have been normalized by the P(90, 90) reference image. Hence, there is no scaling factor invoked in the linear-combination. The consistency of different combinations testifies the quality of data and the robust of this simple inversion method.

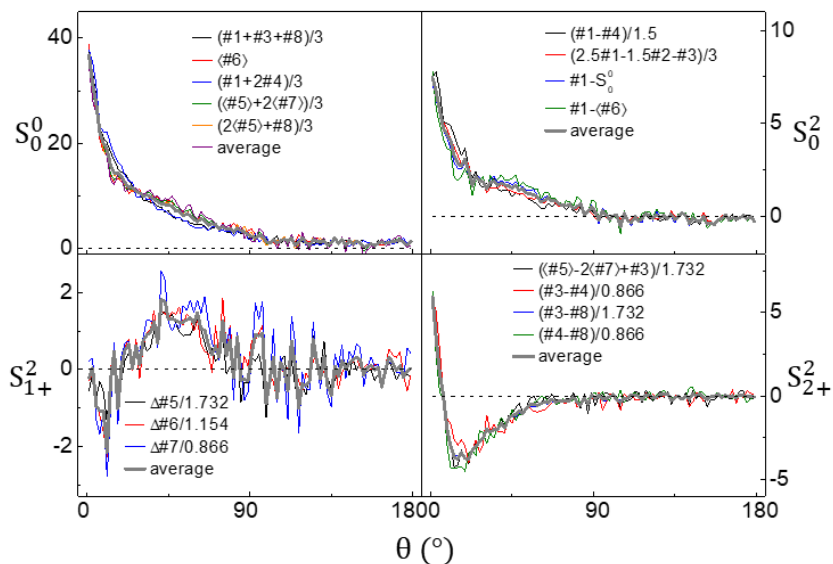


FIG. S4. Same as Fig. S3, except for the HCl($v=1$) product channel at $E_c = 4.8$ kcal mol $^{-1}$.

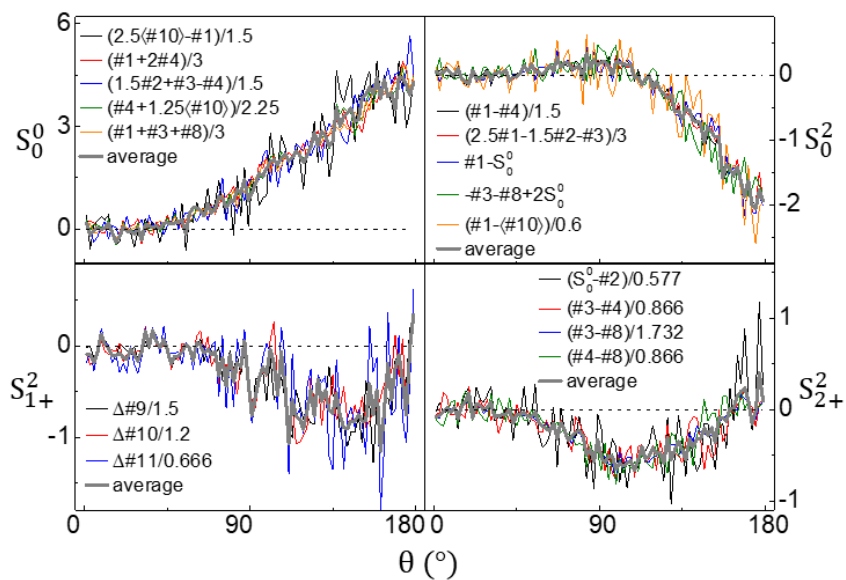


FIG. S5. Same as Fig. S3, except for the HCl($v=0$) product channel at $E_c = 2.7$ kcal mol $^{-1}$.

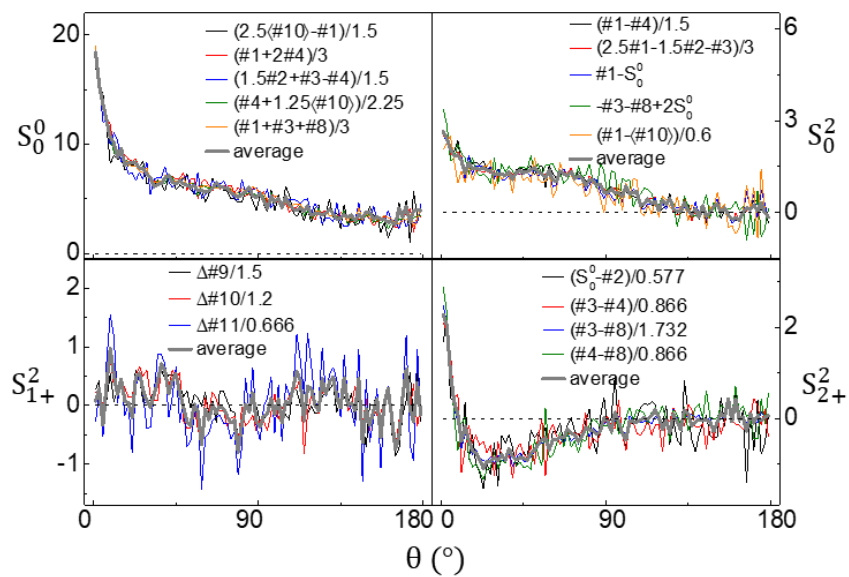


FIG. S6. Same as Fig. S5, except for the HCl($v=1$) product channel at $E_c = 2.7$ kcal mol $^{-1}$.